

Global Linear Instability Analysis of Diffusion-Flame Flickering

Daniel Moreno, Wilfried Coenen, Alejandro Sevilla
Universidad Carlos III de Madrid
28911 Leganés, Spain

Jaime Carpio, Amable Liñán
Universidad Politécnica de Madrid
28006 Madrid, Spain

Antonio L. Sánchez
University of California San Diego
La Jolla, CA 92093-0411, USA

1 Introduction

At sufficiently low Froude numbers, jet diffusion flames are known to undergo a bifurcation to a periodic flow state referred to as “flame flicker” [1]. The associated frequency varies between the values found in laboratory-scale experiments, typically in the range of 10 to 20 Hz, to values as small as 0.5 Hz for large-scale pool fires [2]. The role of buoyancy as the driving mechanism was recognized in the early theoretical analysis of Buckmaster and Peters [3], who postulated that the flickering was associated with a modified Kelvin-Helmholtz instability of the annular flow induced by buoyancy in the envelope of hot gases surrounding the jet flame. By performing an inviscid, parallel flow stability analysis of a simplified self-similar model problem (the so-called infinite candle) they were able to determine an expression for the flicker frequency, which was predicted to vary with the one fourth power of the streamwise distance. This dependence, although weak, was readily recognized as a weakness of the results [4]. As pointed out by Buckmaster and Peters in their 1986 paper [3], a “detailed viscous stability analysis of the complete flow field” could help to examine the validity of the results of their simplified study, although they recognized that the suggested analysis was “a formidable undertaking” at the time. As a result of the increase in computer power and of the development of robust numerical techniques that have occurred in the intervening time, such an analysis can be performed nowadays with reasonable computational cost, that being the purpose of the present work.

While the early theoretical work assumed a convective instability [3], later experimental observations [5] suggested that the flame flickering phenomenon was associated instead with a globally excited oscillation forced by a region of absolutely unstable flow near the base of the jet exit. These findings were later supported by direct numerical simulations [6] and by local linear stability analyses assuming nearly

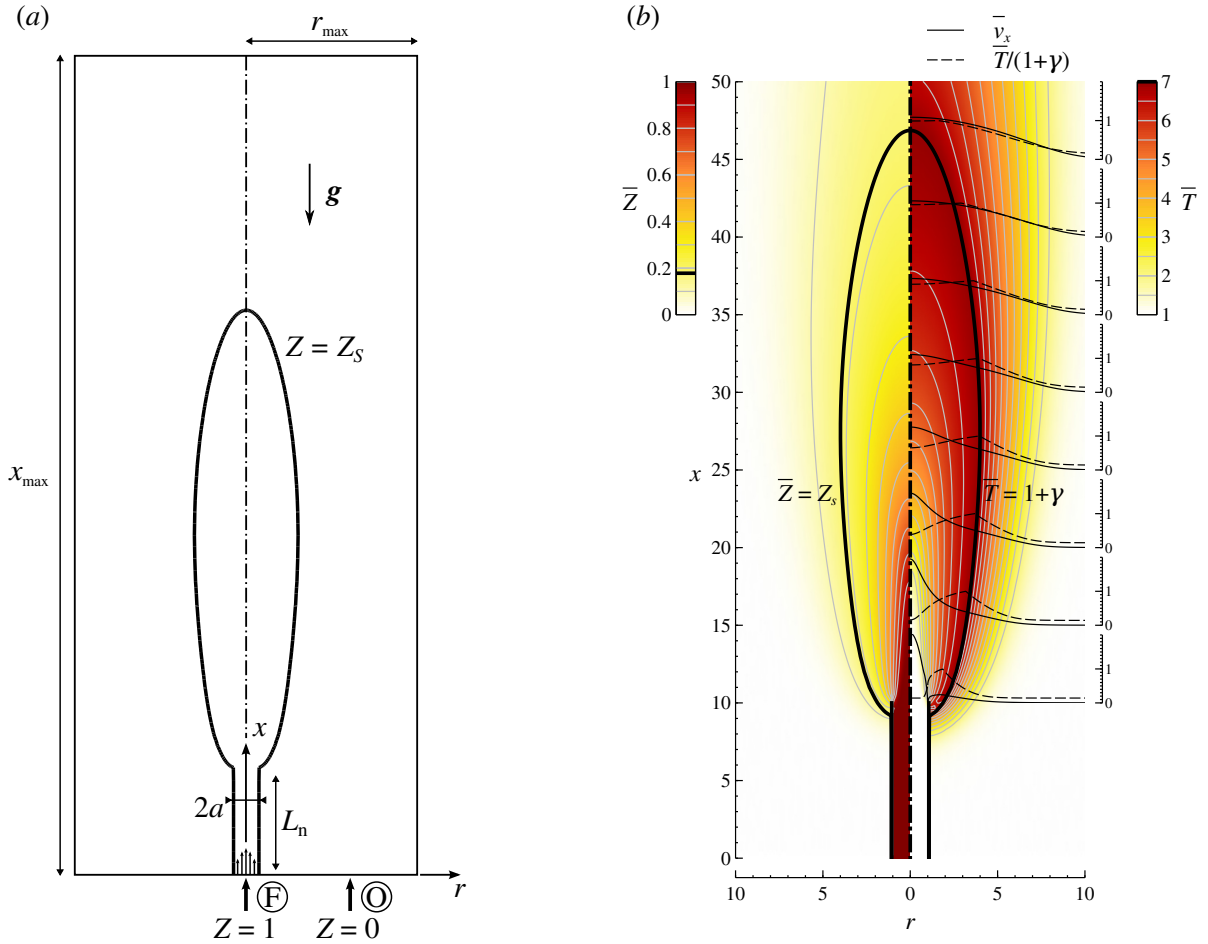


Figure 1: (a) Sketch of the problem and computational domain. (b) Base-flow isocontours of \bar{Z} (left-hand side) and \bar{T} (right-hand side) together with radial profiles of \bar{v}_x and \bar{T} at $x = 10, 15, 20, 25, 30, 40, 45$ for $Pr = 0.7, L_F = 1, S = 4.62, \gamma = 6, T_A = 1, Re = 100$ and $Fr = 625$; the thick solid line represents the stoichiometric flame surface $\bar{Z} = Z_s$, where $\bar{T} = 1 + \gamma$.

parallel flow [7]. The present work is different from these previous attempts, in that it employs, for the first time, a linear global instability analysis to examine buoyancy-induced flickering of axisymmetric laminar jet diffusion flames. The method determines directly, without invoking weakly nonparallel assumptions, the critical conditions at the onset of the linear global instability as well as the Strouhal number of the associated oscillations in terms of the governing parameters of the problem, thereby circumventing the need for analyzing the local convective/absolute stability character of the flow.

2 Problem statement

The configuration analyzed includes a vertical fuel jet with temperature T'_0 and density ρ'_0 discharging upwards through an injector of inner radius a into an infinite air atmosphere at temperature T'_A , as indicated in figure 1(a). For generality, the analysis considers dilution of the fuel with an inert gas, with $Y_{F,0}$ denoting the fuel mass fraction in its feed stream, while $Y_{O_2,A} = 0.232$ is the oxygen mass fraction in air. In the description, focused on the fluid mechanic aspects of the flow, we adopt the one-step irreversible overall reaction $F + sO_2 \rightarrow s_{CO_2}CO_2 + s_{H_2O}H_2O$, according to which the unit mass of fuel reacts with a mass s of oxygen to generate a mass s_{CO_2} of CO_2 and a mass s_{H_2O} of H_2O , with $s_{CO_2} +$

$s_{\text{H}_2\text{O}} = s + 1$, releasing in the process an amount of energy given by $q = h_{\text{F}}^o - s_{\text{CO}_2} h_{\text{CO}_2}^o + s_{\text{H}_2\text{O}} h_{\text{H}_2\text{O}}^o$, where h_i^o denotes the enthalpy of formation per unit mass of species i . The above representation of the underlying stoichiometry for the oxidation of the fuel embodies the fundamental thermochemical parameters involved in nonpremixed flames [8], namely, the mass of air that one needs to mix with the unit mass of the gaseous fuel stream to generate a stoichiometric mixture $S = sY_{\text{F},0}/Y_{\text{O}_2,A}$ and the dimensionless temperature increment resulting from the adiabatic combustion of that mixture $\gamma = (qY_{\text{F},0})/[c_p T'_A(1+S)]$, with c_p representing the specific heat at constant pressure, assumed to be constant in the following analysis. Typical values for undiluted hydrocarbon-air flames are $S = 15$ and $\gamma = 7$.

Often in nonpremixed-combustion applications, the characteristic fluid mechanical time, defined in laminar jet flames by the characteristic residence time a/U_0 , with $U_0 = \dot{m}/(\pi a^2 \rho'_0)$ being the average jet velocity based on the fuel mass flow rate \dot{m} , is much larger than the characteristic time of fuel oxidation in the high-temperature flame region. Under those conditions, the chemical reaction occurs at a fast rate in a very thin layer, outside of which the chemical equilibrium condition

$$\hat{Y}_{\text{F}} \hat{Y}_{\text{O}_2} = 0 \quad (1)$$

applies in the first approximation, $\hat{Y}_{\text{F}} = Y_{\text{F}}/Y_{\text{F},0}$ and $\hat{Y}_{\text{O}_2} = Y_{\text{O}_2}/Y_{\text{O}_2,A}$ representing here the fuel and oxygen mass fractions normalized with their values in their respective feed streams. The resulting flow can be described by considering the limit of infinitely fast combustion, in which the reaction-rate terms in the conservation equations for energy and species appear as Dirac delta distributions located at the flame, which becomes in this limit an infinitesimally thin surface separating a near-axis region without oxygen from a fuel-free outer atmosphere [9]. In the computations below, we use the coupling-function formulation presented in [8], originally developed by Liñán [10], who generalized the Burke-Schumann description of diffusion-controlled combustion to the realistic cases in which the Lewis of the fuel L_{F} is nonunity. The description involves the two mixture-fraction variables

$$Z = \frac{S\hat{Y}_{\text{F}} - \hat{Y}_{\text{O}} + 1}{S + 1} \quad \text{and} \quad \tilde{Z} = \frac{S\hat{Y}_{\text{F}}/L_{\text{F}} - \hat{Y}_{\text{O}} + 1}{S/L_{\text{F}} + 1}, \quad (2)$$

together with the excess-enthalpy variable

$$H = \frac{T - T_A}{T_A} + \frac{\gamma(S + 1)}{S}(\hat{Y}_{\text{O}} - 1), \quad (3)$$

where the nondimensional temperature T has been scaled with T'_0 , with $T_A = T'_A/T'_0$ correspondingly being its value in the surrounding air atmosphere. The standard mixture fraction Z and the diffusion-weighted mixture fraction \tilde{Z} are defined to be zero in the air stream and unity in the fuel stream, respectively, while $H = 0$ in the air stream and $H = H_0 = (1 - T_A)/T_A - \gamma(S + 1)/S$ in the fuel stream. At the flame, where both reactants appear in zero concentrations, the mixture fractions take the stoichiometric values $Z = Z_S = 1/(S + 1)$ and $\tilde{Z} = \tilde{Z}_S = 1/(S/L_{\text{F}} + 1)$.

The low-Mach number approximation is used in the description. Using the jet radius a and the residence time a/U_0 as scales in nondimensionalizing the problem, reduces the conservation equations to

$$\frac{\partial \rho}{\partial t} + \nabla \cdot (\rho \mathbf{v}) = 0, \quad (4)$$

$$\rho \frac{\partial \mathbf{v}}{\partial t} + \rho \mathbf{v} \cdot \nabla \mathbf{v} = -\nabla p + \frac{1}{Re} \nabla \cdot \bar{\tau} + \frac{1}{Fr} (T_A^{-1} - \rho) \mathbf{e}_x, \quad (5)$$

$$\rho \frac{\partial Z}{\partial t} + \rho \mathbf{v} \cdot \nabla Z = \frac{1}{Re Pr} \nabla \cdot \left[\left(\frac{S/L_{\text{F}} + 1}{S + 1} \right) \rho D_{\text{T}} \nabla \tilde{Z} \right], \quad (6)$$

$$\rho \frac{\partial H}{\partial t} + \rho \mathbf{v} \cdot \nabla H = \frac{1}{Re Pr} \nabla \cdot (\rho D_{\text{T}} \nabla H), \quad (7)$$

where p represents the pressure difference from the unperturbed ambient distribution, appropriately non-dimensionalized with its characteristic value $\rho'_0 U_0^2$, $\mathbf{v} = (v_x, v_r)$ is the nondimensional velocity field scaled with U_0 , and $\bar{\tau} = \mu(\nabla\mathbf{v} + \nabla\mathbf{v}^T) + (m_0\mu_B - \frac{2}{3}\mu)(\nabla \cdot \mathbf{v})\bar{I}$ is the viscous stress tensor, with \bar{I} representing the identity tensor. The power-law expressions $\mu = \rho D_T = \mu_B = T^{0.7}$ are employed for the the temperature dependence of the transport coefficients, where ρ , D_T , μ , and μ_B are the nondimensional density, thermal diffusivity, shear viscosity, and bulk viscosity scaled with their values in the fuel jet ρ'_0 , $D'_{T,0}$, μ'_0 , and $\mu'_{B,0}$, with $m_0 = \mu'_{B,0}/\mu'_0$ correspondingly representing the ratio of bulk viscosity to shear viscosity in that stream. The Prandtl number Pr (the ratio of the kinematic viscosity to the thermal diffusivity) is assumed to be constant in the description. Equations (4)–(7) must be supplemented with the equation of state $\rho T = 1$, which is written for simplicity neglecting the variations of mean molecular weight in the gas mixture, and with the expressions

$$\hat{Y}_O = 0, \quad Y_F = \frac{Z - Z_S}{1 - Z_S} = \frac{\tilde{Z} - \tilde{Z}_S}{1 - \tilde{Z}_S}, \quad \text{and} \quad \frac{T - T_A}{T_A} = H + \frac{\gamma}{1 - Z_S}, \quad \text{for } Z \geq Z_S, \quad (8a)$$

$$Y_F = 0, \quad \hat{Y}_O = 1 - \frac{Z}{Z_S} = 1 - \frac{\tilde{Z}}{\tilde{Z}_S}, \quad \text{and} \quad \frac{T - T_A}{T_A} = H + \frac{\gamma}{1 - Z_S} \frac{Z}{Z_S} \quad \text{for } Z \leq Z_S, \quad (8b)$$

obtained from the definitions (2) and (3) with use made of the equilibrium condition (1).

The boundary conditions for the integration of (4)–(7) include a symmetry condition along the axis. The values of the coupling functions are specified at the nozzle inlet and in both the air region and the lateral boundary. As for the velocity, a Poiseuille distribution, $\mathbf{v} = 2(1 - r^2)\mathbf{e}_x$, is assumed upstream from the injector exit, while a condition of vanishing stress is used on the lateral boundary $r = r_{\max}$ and also downstream at $x = x_{\max}$. No forced air coflow is considered in the integrations below, so that the air enters the domain as needed to satisfy the jet-entrainment requirements.

Besides the transport numbers Pr and L_F , the thermochemical parameters S and γ (the former appearing through the stoichiometric values Z_S and \tilde{Z}_S in (8)), and the ambient-temperature ratio T_A , the formulation displays two controlling fluid mechanical parameters, namely, the Reynolds number $Re = \rho'_0 U_0 a / \mu'_0$ and the Froude number $Fr = U_0^2 / (g a)$. The computations shown below correspond to $m_0 = 0$, $Pr = 0.7$, $L_F = 1$, $S = 4.62$, $\gamma = 6$ and $T_A = 1$ for different values of Re and Fr .

The equations were linearized around the base flow with use made of the normal-mode decomposition

$$(\mathbf{v}, p, Z, H) = (\bar{\mathbf{v}}, \bar{p}, \bar{Z}, \bar{H})(x, r) + (\hat{\mathbf{v}}, \hat{p}, \hat{Z}, \hat{H})(x, r)e^{-i\omega t}, \quad (9)$$

leading to a nonlinear set of equations for the base flow $(\bar{\mathbf{v}}, \bar{p}, \bar{Z}, \bar{H})$ (i.e., the steady counterpart of (4)–(7)), and an accompanying set of linear equations,

$$i\omega\mathcal{B}\hat{\mathbf{q}} = \mathcal{L}\hat{\mathbf{q}}, \quad (10)$$

for the eigenfunctions $\hat{\mathbf{q}} = (\hat{\mathbf{v}}, \hat{p}, \hat{Z}, \hat{H})$, with the complex angular frequency $\omega = \omega_r + i\omega_i$ emerging as an eigenvalue of the problem. The real part of ω is the frequency of the perturbation, and is related to the associated Strouhal number through $St = \omega_r / \pi$; the imaginary part is the growth rate, and dictates whether the flame is globally stable, $\omega_i < 0$, or unstable, $\omega_i > 0$.

The equations were discretized using the finite-element software FreeFEM++ on the cylindrical domain depicted in figure 1(a). The system of equations for the base flow is solved using a Newton-Raphson method. The discretized version of the generalized eigenvalue problem (10) is solved using a shift-invert method (see, for instance [11]). The radial extent of the domain was chosen to be $r_{\max} = 40$; increasing this value further was checked to have a negligible influence on the results. The streamwise extent of the domain, x_{\max} , was also varied. For the computations shown below, it was found that any choice

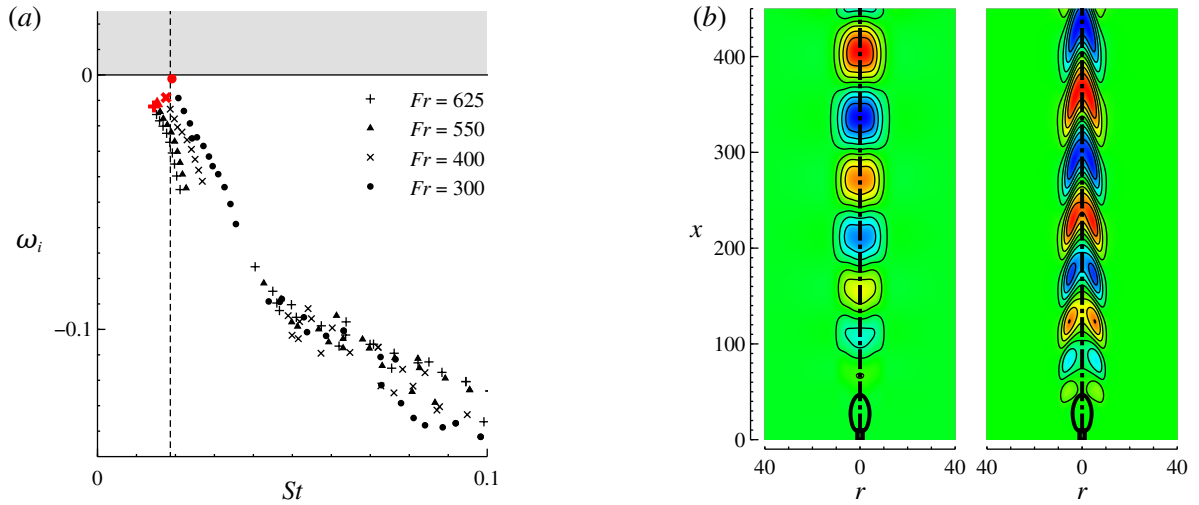


Figure 2: (a) Eigenvalue spectra for $Pr = 0.7$, $L_F = 1$, $S = 4.62$, $\gamma = 6$, $T_A = 1$, $Re = 100$, and $Fr = 300, 400, 550, 625$. (b) Real part of the streamwise velocity \hat{v}_x (left) and mixture fraction \hat{Z} (right) for the eigenfunctions of the most unstable mode with $Re = 100$ and $Fr = 300$.

of $x_{\max} > 450$ gives almost identical results for the base flow as well as for the most unstable mode (that with the largest ω_i), so that the numerical scheme is able to provide with sufficient accuracy both the critical conditions for the onset of the instability, corresponding to $\omega_i = 0$, as well as the frequency ω_r of the resulting oscillations. By way of contrast, all other eigenmodes in the resulting spectra were found to be very dependent on the domain length, even up to $x_{\max} = 450$, a characteristic of the solution arising also in isothermal-jet computations [11].

3 Sample results

The typical structure of the basic flow is presented in figure 1(b) for the case $Re = 100$ and $Fr = 625$, including isocontours of \bar{Z} and \bar{T} . Radial profiles of axial velocity \bar{v}_x and temperature \bar{T} are shown on the left-hand side at different axial positions. A thick solid curve is used to denote the flame location, where $\bar{Z} = Z_s$ and $\bar{T} = 1 + \gamma$. Buoyancy is seen to accelerate the flow in the flame envelope, promoting the instability through the increased shear and the appearance of inflection points in the velocity profile on both sides of the flame. Also essential for the instability is the action of the baroclinic torque induced by the strong radial temperature—or density—gradient around the inflection points. This effect, which is known to play a key role in the stability of inhomogeneous mixing layers [13] and low-density jets [14], can be expected to be also essential for diffusion-flame flickering.

Figure 2(a) shows the computed eigenvalue spectra for $Re = 100$ and $Fr = 300, 400, 550, 625$. For all cases, the most unstable eigenmode is indicated with a bigger symbol in red. Decreasing the Froude number is seen to destabilize the flow, with marginally stable conditions reached for $Fr = 300$. Further decreasing Fr would trigger the onset of a global instability mode in the flame, which would start oscillating at a frequency $St = 0.0191$. The accuracy of this prediction was tested by comparing with results of a direct numerical simulation for $Re = 100$ and $Fr = 300$. The resulting periodic solution, generated with a time-dependent axisymmetric code developed earlier [12], was seen to exhibit oscillations with $St = 0.0187$ (dashed line of figure 2(a)). The spatial structure of the marginally stable eigenmode is shown in figure 2(b). The typical wavelength is seen to be of the order of 100 radii.

The instability analysis outlined above was also used to investigate effects of Reynolds number on

the global stability of the flame. As expected, increasing the Reynolds number has a destabilizing effect, in agreement with what is observed in low-density jets. It was found that the critical value of Re increases for increasing values of the Froude number and that nonbuoyant flames ($Fr \rightarrow \infty$) are globally stable up to the largest Reynolds number $Re = 2000$ considered in the computations. Clearly, additional dependences of the stability threshold on the thermochemical parameters γ and S are also worth investigating to clarify influences of exothermicity and fuel dilution.

References

- [1] Chamberlin DS, Rose A. (1948) The flicker of luminous flames. *Proc. Combust. Inst.* 1–2:27–32.
- [2] Schoenbuecher A, Arnold B, Banhardt K, Bieller V, Kasper H, Kaufmann M, Lucas R, and Schiess N. (1986) Simultaneous observation of organised density structures and the visible field in pool fires. *Proc. Combust. Inst.* 21:83–92.
- [3] Buckmaster J, Peters N. (1986) The infinite candle and its stability– a paradigm for flickering diffusion flames. *Proc. Combust. Inst.* 21:1829–1836.
- [4] Mahalingam S, Cantwell BJ, and Ferziger JH. (1991) Stability of low-speed reacting flows. *Phys. Fluids A*, 3:1533–1543.
- [5] Maxworthy T. (1999) The flickering candle: transition to a global oscillation in a thermal plume. *J. Fluid Mech.* 390:297–323.
- [6] Jiang X, Luo KH. (2000) Combustion-induced buoyancy effects of an axisymmetric reactive plume. *Proc. Combust. Inst.* 28:1989–1995.
- [7] See YC, Ihme M. (2014) Effects of finite-rate chemistry and detailed transport on the instability of jet diffusion flames. *J. Fluid Mech.* 745:647–681.
- [8] Liñán A, Vera V, Sánchez AL. (2015) Ignition, liftoff, and extinction of gaseous diffusion flames. *Ann. Rev. Fluid. Mech.* 47:293:314
- [9] Burke SP, Schumann TEW. (1928) Diffusion flames. *Ind. Eng. Chem.* 20:998–1004.
- [10] Liñán A (1991) The structure of diffusion flames. In *Fluid Dynamical Aspects of Combustion Theory*, ed. Monofri, A Tesev, pp. 11–29. Harlow, UK: Longman Sci. Tech.
- [11] Garnaud, X., Lesshafft, L., Schmid, P., Huerre, P. Modal and transient dynamics of jet flows. *Physics of Fluids* 2013. 25:044103
- [12] J. Carpio, J.L. Prieto. An anisotropic, fully adaptive algorithm for the solution of convection dominated equations with semi-Lagrangian schemes. *Computer Methods in Applied Mechanics and Engineering*, Vol. 273 (2014), pp. 77 - 99.
- [13] Soteriou M. C., Ghoniem A. F. (1995) Effects of the free-stream density ratio on free and forced spatially developing shear layers. *Phys. Fluids* 7, 2036.
- [14] Lesshafft L., Huerre P. (2007) Linear impulse response in hot round jets. *Phys. Fluids* 19, 024102.